

Cyclic loading response of footing on multilayered rubber-soil mixtures

S.N. Moghaddas Tafreshi^{*1a} (Corresponding Author), N. Joz Darabi^{1b}, A.R. Dawson^{2c}

¹*Department of Civil Engineering, K.N. Toosi University of Technology, Valiasr St., Mirdamad Cr., Tehran, Iran,*

²*Nottingham Transportation Engineering Centre, University of Nottingham, Nottingham, UK.*

Abstract. This paper presents a set of results of plate load tests that imposed incremental cyclic loading to a sandy soil bed containing multiple layers of granulated rubber-soil mixture (RSM) at large model scale. Loading and unloading cycles were applied with amplitudes incrementally increasing from 140 to 700 kPa in five steps. A thickness of the RSM layer of approximately 0.4 times the footing diameter was found to deliver the minimum total and residual settlements, irrespective of the level of applied cyclic load. Both the total and residual settlements decrease with increase in the number of RSM layers, regardless of the level of applied cyclic load, but the rate of reduction in both settlements reduces with increase in the number of RSM layers. When the thickness of the RSM layer is smaller, or larger, settlements increase and, at large thicknesses may even exceed those of untreated soil. Layers of the RSM reduced the vertical stress transferred through the foundation depth by distributing the load over a wider area. With the inclusion of RSM layers, the coefficient of elastic uniform compression decreases by a factor of around 3-4. A softer response was obtained when more RSM layers were included beneath the footing damping capacity improves appreciably when the sand bed incorporates RSM layers. Numerical modeling using “FLAC-3D” confirms that multiple RSM layers will improve the performance of a foundation under heavy loading.

Keywords: Cyclic loading, multiple RSM layers, residual and resilient settlements, coefficient of elastic uniform compression (CEUC), Numerical analysis

1. Introduction

In recent decades, the volume of scrap tire rubber being generated in the world has become significant because of developing industry and growing population (WRAP, 2007; RMA, 2007; RRI, 2009). As this waste stream has accumulated, its disposal has, therefore, become a major environmental problem worldwide of waste tires are either dumped in landfills or stockpiled across the landscape in huge volumes (Cetin et al., 2006; Chiu, 2008). It makes them harder and more expensive to dispose of safely without threatening human health and environment. For instance, stockpiled waste

*Corresponding author, Professor, E-mail: nas_moghaddas@kntu.ac.ir

^aProfessor, E-mail: nas_moghaddas@kntu.ac.ir

^bPh.D. Candidate, E-mail: naser_darabi@yahoo.com

^cAssociat Professor, Email: andrew.dawson@nottingham.ac.uk

tires are flammable, prone to fires with toxic fumes and may then cause a major health hazard for both human beings and animals (Attom, 2006).

In consideration of the environmental concerns, and due to a greater willingness to use alternative sources, the use of waste tires in the form of strips, chips, granules, crumbs or shreds, are now considered as construction materials (Tanyu et al. 2004; Ghosh and Dey 2009; Consoli et al. 2009; Edinçliler and Avhan 2013; Moghaddas Tafreshi et al. 2012; Edinçliler and Cagatay, 2013). When the chipped, shredded and granulated tire rubbers are mixed with soil (or the strips of tire used as reinforcement), the mixture can behave as reinforced soil, similar to geosynthetic- or fiber- reinforced soil, which can be advantageously employed to increase soil strength, depending on the rubber content and the size of rubber particles (Hataf and Rahimi 2005; Yoon et al., 2006; Tavakoli Mehrjardi et al., 2012; Edinçliler and Cagatay 2013). The cyclic load response of rubber-soil mixtures has shown the material's potential as a composite material, particularly in applications in roads, highways, and embankments (e.g. as identified by Bosscher et al., 1997; Feng and Sutter 2000; Edinçliler et al., 2004; Prasad and Prasad Raju, 2009; Moghaddas Tafreshi and Norouzi, 2015; Brara, 2016).

Bosscher et al. (1997) used tire-chips in soil to form a laboratory model embankment which was then subjected to simulated, repeated loads. Less surface plastic displacement was reported when the tire-chips were covered by a relatively thick soil-only layer than when the tire-chips were placed in the whole of the fill. The soil cap over the tire-chips not only reduces the on-going settlement, but also limits access to oxygen, hindering tire shreds from ignition (Attom, 2006). Yoon et al. (2006) evaluated the feasibility of using tire shred-sand mixtures as a fill material in embankment construction. A test embankment was constructed using a 50/50 mixture, by volume of tire shreds and sand. They reported that, after 200 days of road traffic, the settlement stabilized at small values when compared with layers of pure tire shreds and pure sand. Edinçliler and Cagatay (2013) investigated the feasibility of reinforcing soil with extensible buffering rubber inclusions by observing the CBR performance of the mixtures. They reported that adding 5% of fiber-shaped buffering rubber by weight to sand formed a reinforced composition for use in geotechnical applications, improving the CBR value of soil.

Several investigations have highlighted the beneficial use of rubber-soil mixture (as a single layer or as a large mass of rubber-soil mixture) in construction of foundations bed, embankments and retaining wall (Bosscher et al. 1997; Yoon et al., 2006; Hataf and Rahimi, 2005; Moghaddas Tafreshi and Norouzi, 2012; 2015; Dammala et al., 2015; Reddy and Murali Krishna, 2015; 2016). Yet the effectiveness of a multi-layered rubber-soil mixture subjected to load-unload-reload cycles at increasing stress levels (termed incremental cyclic loading in this paper) used in the zone significantly stressed by the footing (which may be over a depth of 1-2 times the loading surface size (i.e. diameter/width) beneath the surface), has not been investigated in recent researches. With the evident benefit of using multiple geotextile, geogrid, or geocell layers (e.g. Sitharam and Sireesh, 2005; Ahmadi and Hajjalilue-Bonab, 2012; Demir et al., 2014; Moghaddas Tafreshi et al., 2014), the use of multiple rubber-soil mixture layers (RSM layers) could be effective, to improve the behaviour of foundation beds under cyclic loading.

2. Aims

This paper seeks to characterize the beneficial effect of vertically-spaced RSM layers in a foundation bed which would have application, potentially, to roads, highways, embankments, machine foundations and pavement foundations. A total of 8 independent incremental cyclic loading tests (plus 12 repeated tests) of a foundation supported on untreated soil or soil containing RSM layers were performed. Testing was arranged so as to determine the parameters controlling best usage. However, the main objective of the present study is to determine the optimal thickness of RSM layers (h_{rs}) and the effects of the number of RSM layers (N) on settlement response of foundation bed. Also, the effect of the RSM layers on the stress distribution with depth, the damping ratio and the coefficient of elastic uniform compression ($CECU$) were investigated. In addition to plate load tests, numerical results of untreated beds and foundation beds containing 1, 2 or 3 RSM layers were compared with the tests results. Using the validated model, the stress distribution and deformation propagation below the footing for different cases, which may not be easily achievable using the physical model, were obtained.

3. Test Materials

3.1. Backfill soil

A sandy soil passing through the 38 mm sieve (see Fig. 1) with a specific gravity, G_s , of 2.6 was used for the testing program. The soil is classified as well-graded sand, and symbolized as SW in the Unified Soil Classification System (ASTM D 2487-11). Modified proctor compaction tests were performed on the soil, following ASTM D 1557-12. The maximum dry unit weight was 20.62 kN/m^3 , with an optimum moisture content of 5.7%. The angle of internal friction (ϕ) of the soil, obtained by consolidated undrained triaxial compression tests at a bulk unit weight of 18.52 kN/m^3 (corresponding to 85% of maximum dry unit weight, similar to the compacted density of soil layers in backfill in Section 4.2) of specimens contain gravel size grains, was 39.5° . This soil was used for untreated layers and to mix with rubber for construction of the RSM layers.

3.2. Rubber

The particles of granulated tire rubber used in the test program had a specific gravity, G_s , of 1.17. They were between 2 mm and 25 mm in size and had a mean particle size of 14 mm. These particles had non-spherical shapes and were clean and free of any steel and cord. Fig. 1 and Fig. 2 show, respectively, the grading and a photograph of the rubber particles used in the tests. When required, to form the combined rubber and soil mixtures (i.e. RSM), the rubber particles were carefully blended into the soil, by weight using a pan mixer, with manual intervention if necessary, so as to produce a reasonably uniform, non-segregated, rubber-soil mixture. To control and check the uniform distribution of the rubber particles in mixture, three samples of the mixture with specified weight were collected from different parts of the mix volume. By passing the samples through a sieve, rubber particles and soil particles were separated and then the rubber content was measured. The results show a close match between the measured rubber contents and target rubber content with maximum differences less than 0.6%. The consistency and close match between assessments (see Section 5)

demonstrates that the use of mixer and mixture procedure delivered a consistent product without causing damage to the rubber that would affect performance.

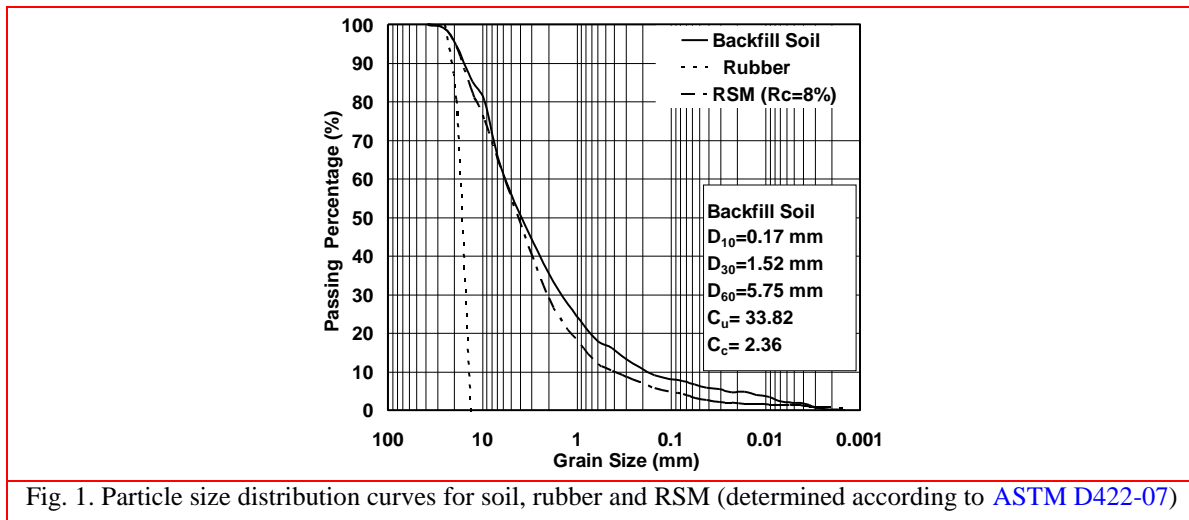


Fig. 1. Particle size distribution curves for soil, rubber and RSM (determined according to [ASTM D422-07](#))

The authors recognize that the production of such a uniform mixture of soil and rubber might not be easily reproduced in the field in regular practice and might, therefore, require special mixing procedures. For this reason, the results obtained in the test program reported here may be regarded as yielding the maximum credible benefit of any large-scale implementation.



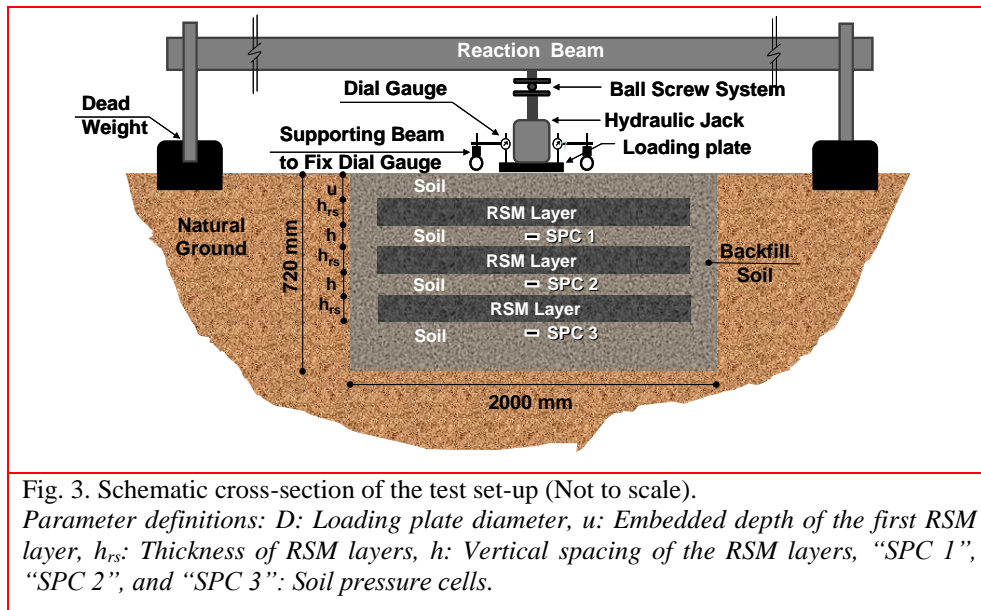
Fig. 2. A view of the granulated tire rubber

3.3. Rubber-Soil Mixture (RSM)

In all tests containing RSM layers, granulated rubber was used at a mass replacement rate of 8% ($R_c=8\%$) by weight (Moghaddas Tafreshi et al., 2013) in the middle of the rates of 6% and 10% recommended, respectively, by Prasad and Prasada Raju (2009) and Munnoli et al (2013). The maximum and minimum void ratio (e_{max} and e_{min}) and specific gravity, G of RSM were obtained as 0.92, 0.32 and 2.36, respectively. Fig. 1 shows the grading of the rubber soil mixture (RSM) particles with rubber content of 8% ($R_c=8\%$). The rubber content has a significant influence on unit weight and shear strength of mixture, as with an increase in rubber percentage, shear modulus and unit weight decrease (Nakhaei et al., 2012.).

4. Full scale model test

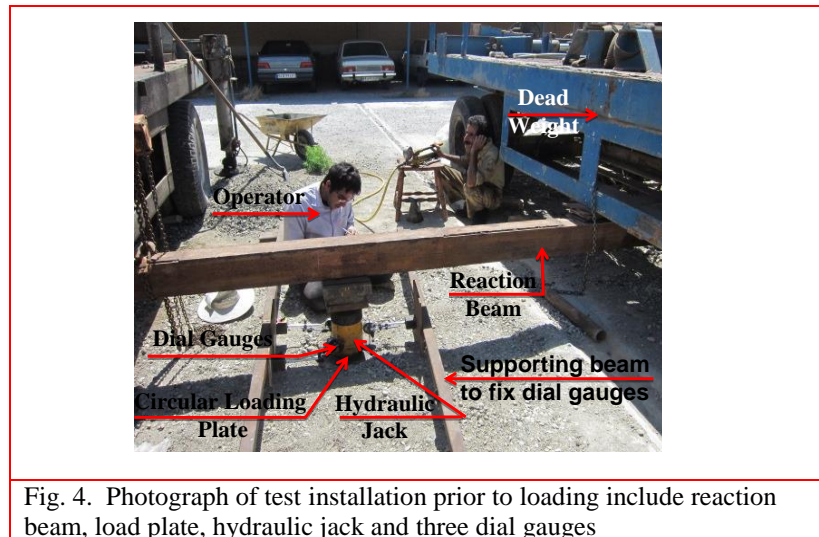
To provide relative realistic test conditions, to investigate any performance improvement in the deformation response and also to determine the stress distribution across the depth of the foundation bed, a full-scale model test using standard plate loading was conducted. The schematic cross-section of the test set-up of the foundation bed containing a model test pit trench, layers of the backfill soil, RSM layers, the loading plate, loading system and data measurement system (dial gauges and three soil pressure cells (abbreviated to “SPC 1”, “SPC 2”, and “SPC 3” inside the foundation bed) and the geometry of the test configurations, is shown in Fig. 3.



4.1. Test pit and instrumentation

All plate load tests were conducted in an outdoor test pit (see Acknowledgements). The test pit, measuring 2000 mm × 2000 mm in plan, and 720 mm in depth, was excavated in natural ground so as to construct the soil layers, RSM layers and to install three pressure cell at specified depths. The load application system was a hydraulic jack imposed by a manually-operated pump and supported against a strong reaction beam spanning the width of the test pit. The dead weight used to support the reaction beam was provided by two light trucks (Fig. 4). A steel, rigid, circular plate of 300 mm in diameter and 25.4 mm in thickness was placed on the surface at the center of the installation as a model footing. The diameter and thickness of the loading plate were selected according to the [ASTM D1196-04](#) and [ASTM D1195-09](#). These standards indicate a circular steel plate should be used not less than 25.4 mm in thickness and with a diameter between 150 and 750 mm.

To measure the movement of the plate throughout the tests, three linear dial gauges with an accuracy of 0.01% of full range (100 mm) were attached to a reference beam and their tips placed about 10 mm inwards from the edge of the plate. Also, to measure the vertical stress inside the foundation bed, it was instrumented with three full bridged, 50 mm diameter diaphragm-type soil pressure cells (abbreviated to SPC). These had an accuracy of 0.01% of full range of 1000 kPa according to the manufacturer. The top soil pressure cell (abbreviated to “SPC 1”), middle soil pressure cell (SPC 2”), and bottom soil pressure cell (“SPC 3”) are located, respectively, at 210 mm, 390 mm and 570 mm beneath the center of loading plate (Fig. 3). The pressure cells’ output was recorded in mV and then converted to stress units using calibrations obtained as described below. In order to prevent damage to the soil pressure cells (SPC), they were only installed for Test Series 1 and 3 (i.e. for the foundation beds with one layer of RSM; in Test Series 2, no pressure cells were installed, see Table 1). A photograph of the test installation prior to testing, showing the reaction beam, load plate, hydraulic jack and three dial gauges is presented as Fig. 4.



To ensure an accurate pressure reading, the three pressure cells were calibrated prior to each test series. This was achieved in a 300 mm-diameter and 200 mm-high cylinder container made of very

soft textile filled with the soil. Each cell was placed, in turn, in the middle of this container. The container was then placed in a compression machine and the cells were calibrated for different levels of applied pressure.

4.2. Backfill compaction

In order to compact the layers of the foundation, including both soil and RSM layers, a walk-behind vibrating plate compactor, 450 mm in width, was used. The soil layers and RSM layers were provided at a thickness of 60 mm and at an optimum moisture content of 5.7%. To achieve the required density of backfill layers, in all the tests, the soil layers and RSM layers were compacted with one and three passes, respectively so that the compactive effort, and consequently compaction energy, was kept the same for each pass of the compactor. To better assess the layers' compaction, three sand cone tests in accordance with [ASTM D 1557-12](#) were conducted in some installations and after layer compaction, to measure the densities and moisture content of compacted soil layers and RSM layers.

The unit weight values of RSM layers measured in the three cone tests revealed a close match, with rather small maximum differences of only 1-1.8%. The average measured (recovered) moisture content of the layers was between 5.4% and 5.8%. To prevent loss of moisture from the backfill during the load test, the exposed backfill was covered to a distance of 1.8 m from the circumference of the bearing plate with a waterproof paper. The average (from three sand cone tests) measured dry densities of the soil and of the RSM mixture after compaction were about 17.52 kN/m³ (approximately 85% of maximum soil dry density) and 13.6 kN/m³, respectively.

4.3. Loading system and loading pattern

The load application system was a hand operated hydraulic jack, supported against a strong reaction beam spanning the width of the test pit, with the capability of applying a stepwise controlled load up to 50 kN. In all tests, the maximum applied pressure of 700 kPa was divided into five stages: 140, 280, 420, 560 and 700 kPa. For each stage, only one cycle of loading ($q_{cycl.}$) and unloading, at a rate of 1.5 kPa per second, was applied to the surface of loading plate. Therefore the loading incrementally increased until it reached the desired pressure. Afterwards, the loading and unloading continued at the next level, until the maximum stress was applied. Performance data, i.e. values of pressure at depth and footing settlement, were recorded both during compression and rebound phases. This sequential loading and unloading made it possible to separate the recoverable component (elastic) and non-recoverable component (residual plastic) of the loading plate settlement for different cyclic load levels. The recovered component is often termed "elastic" in the literature, as hereafter in this paper, although the hysteresis evident in each load-unload cycle means that energy is lost during a cycle preventing the response from being fully elastic and a more correct description of the response exhibited would be "elastic hysteresis".

5. Test program

To investigate the beneficial effect of RSM layers on the behaviour of the foundation bed, three test series containing zero (untreated: Test Series 1), one, two and three layers of RSM (Test Series 2 and 3) were conducted. Table 1 gives the details of the tests. Test Series 1 provided reference, untreated, performance data. Test Series 2 were performed to obtain the optimum value of the thickness of RSM layers (h_{rs}/D) using one layer of RSM. The beneficial effect of second and third layers of RSM ($N=1, 2, 3$) is examined in Test Series 3. Test Series 2 and 3, containing RSM layer(s), used layers of mixture placed at $u/D=h/D=0.2$ (according to Yoon et al. (2008) for multi-layered ‘Tirecell’-reinforcement and Moghaddas Tafreshi et al. (2013) for multi-layered geocell reinforcement). The parameter of “ u ” and “ h ” are the depth of the first layer of RSM beneath the loading plate, and the thickness of the soil layer between the RSM layers, respectively. The width of the RSM layers (b) is expressed in non-dimensional form with respect to loading plate diameter ($D=300\text{ mm}$) as, b/D . In line with the findings of Yoon et al., (2008) for multi-layered ‘Tirecell’-reinforcement and Moghaddas Tafreshi et al. (2013) for multi-layered geocell reinforcement, the parameter b/D was held constant in all the tests at $b/D=5$. Greater b/D leads to inefficiency as the lower reinforcement layers are displaced below the depth of influence of the loaded footing and, hence, become ineffective. Less b/D leads to inefficiency as little additional reinforcement effect is experienced for considerably more reinforcing material.

In order to assess the utility of the apparatus, the accuracy of the measurements, the repeatability of the system, the reliability of the results and finally to verify the consistency of the test data, many of the tests described in Table 1 were repeated at least twice. The results obtained revealed a close match between results of the two or three trial tests with maximum differences in results of around 3-6%. This difference was considered to be small and is subsequently neglected. The consistency of the results demonstrates that the mixture of soil and rubber, the test procedure and technique adopted can produce repeatable tests within the bounds that may be expected from geotechnical and pavement testing apparatus.

Test Series	Type of foundation bed	Values of parameters studied in tests			No. of Tests	Purpose of the tests
		$q_{cycl.}$ (kPa)	N	h_{rs}/D		
1	Untreated (Soil only)	140, 280, 420, 560, 700	---	----	1+1*	To quantify the improvements in Test Series 2 and 3
2	Containing RSM layer(s)		1	0.2, 0.4, 0.6, 0.8	4+5*	
3			2, 3	0.4	2+4*	To determine the effect of number of RSM layers

*The tests which were performed two or three times to verify the repeatability of the test data

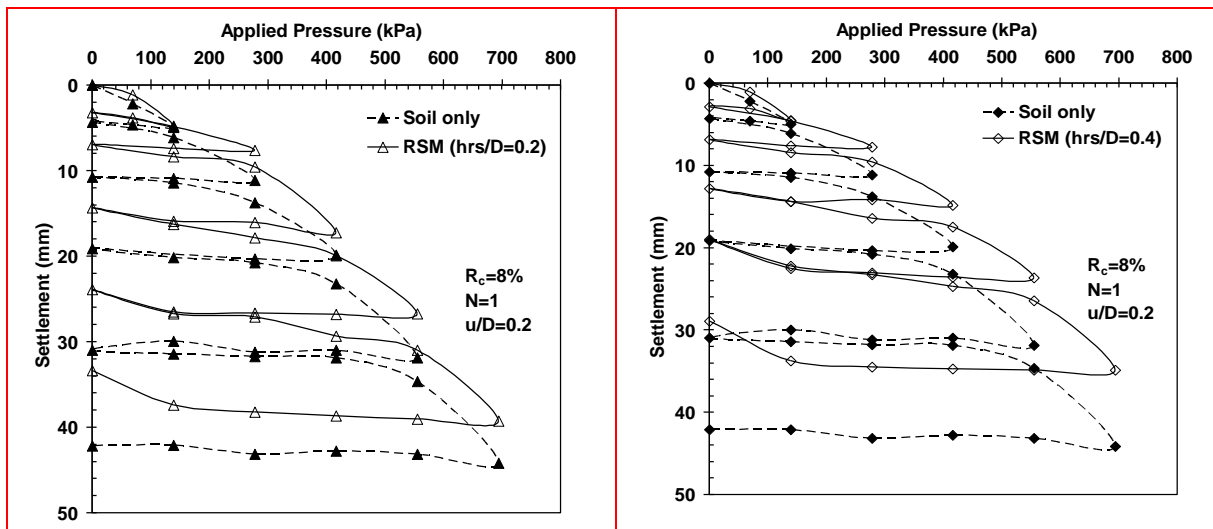
For example, in test Series 2, a total of 9 tests were performed including 4 independent tests plus 5 replicates.

6. Results and discussion

In this section, the results of the incremental cyclic plate load tests are presented along with a discussion highlighting the effects of the thickness of RSM layers on the variations in the plate settlement and the number of RSM layers on the variations in the plate settlement, the distributed pressure at depth of the foundation beds, damping ratio and the Coefficient of Elastic Uniform Compression of soil (abbreviated to CEUC).

6.1. The effect of the thickness of RSM layer (h_{rs}/D ratio)

Fig. 5 compares the pressure-settlement response obtained from incremental cyclic loading and unloading tests of the untreated bed (Tests Series 1) with that of the beds containing a single RSM layer (Tests Series 2) varying the thickness of RSM, h_{rs}/D , and placing the layer at a depth of 0.2 ($u/D=0.2$) from the base of the loading plate. From this figure, it can clearly be observed that in each stage of loading and unloading, a small amount of settlement is recovered ('elastic') while a major part of the settlement remains in the system (plastic) and with increase in the amplitude of loading, the permanent plastic settlements are accumulated gradually. The figure also demonstrates that replacing the portion of untreated soil beneath the footing with a RSM layer, (mostly) decreases both the total (peak) and plastic settlements (residual) of the loading plate, compared with the response of the untreated bed, irrespective of the thickness of mixture layer, h_{rs}/D and the level of applied cyclic load. Fig. 5 also reveals the greater hysteretic nature of the RSM compared to the soil alone. Note how, on unloading, the settlement of the RSM reduces as the applied surface stress drops from peak of cyclic loading (e.g. 560 kPa) to zero whereas the settlement in the soil alone barely changes. This indicates the energy storage and subsequent release achieved by the RSM but not by the soil alone.



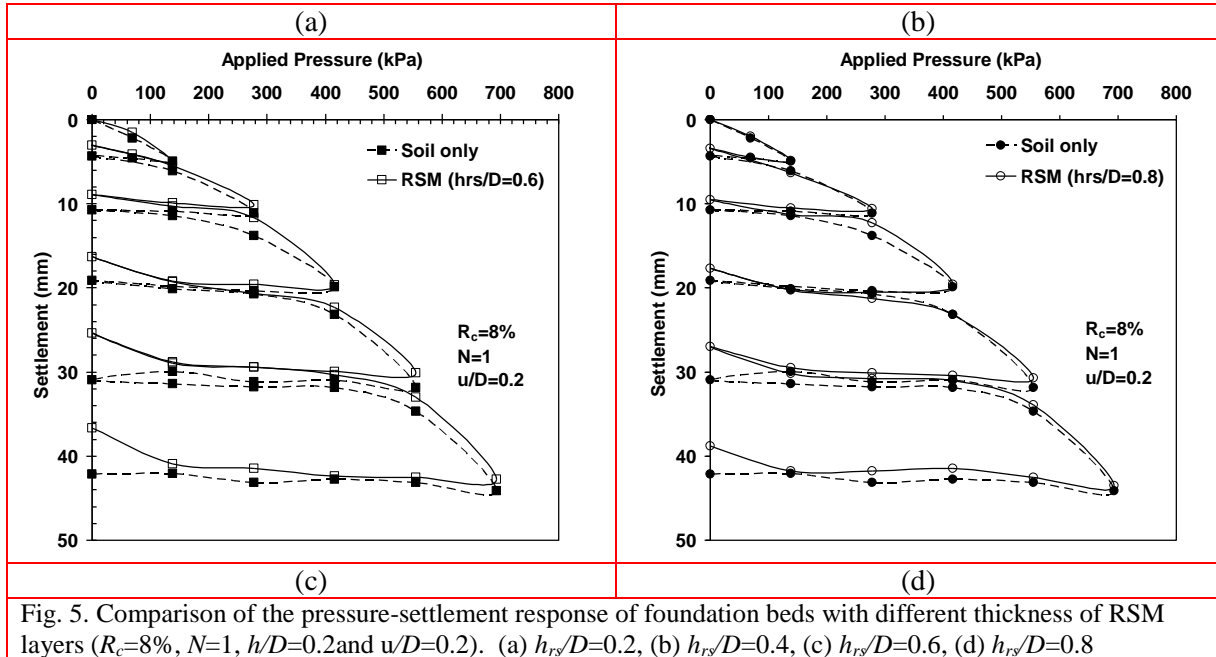


Fig. 5. Comparison of the pressure-settlement response of foundation beds with different thickness of RSM layers ($R_c=8\%$, $N=1$, $h/D=0.2$ and $u/D=0.2$). (a) $h_{rs}/D=0.2$, (b) $h_{rs}/D=0.4$, (c) $h_{rs}/D=0.6$, (d) $h_{rs}/D=0.8$

For a more quantitative comparison, and to show more clearly the effect of the RSM layer on the behaviour of foundation bed, plots of the peak settlement and residual plastic settlement at all applied cyclic load levels, with the thickness of mixture layer, h_{rs}/D are shown in Fig. 6. The results in Figs. 5 and 6 depict that the maximum and residual settlements are considerably decreased up to the value of $h_{rs}/D=0.4$, after which, with further increase in h_{rs}/D ratio to 0.8, their values are increased, regardless of the level of applied cyclic load. For example, from Fig. 6b at 420 kPa amplitude of applied load, the residual settlement values are about 19.1, 14.33, 12.78, 16.31 and 17.72 mm for h_{rs}/D values of zero (i.e. untreated bed), 0.2, 0.4, 0.6 and 0.8, respectively. This example clearly shows the important role of the optimum thickness of RSM layer (h_{rs}/D) inside the foundation bed in decreasing the residual plastic settlement in Fig. 6b and also the total settlement, in Fig. 6a. The maximum increase in performance improvement with $h_{rs}/D=0.4$ could be due to the reinforcement and damping effects of the RSM layer beneath the footing (Prasad and Prasad Raju 2009; Edinliler et al. 2013; Moghaddas Tafreshi and Norouzi, 2012, 2015). Although the reason for the increase in settlement, when the optimum thickness of RSM layer is exceeded, might not be very clear, a large thickness of RSM can make the system response much softer (Zheng and Sutter, 2009; Moghaddas Tafreshi and Norouzi, 2012). This may be a consequence, when rubber is included, of the increased soil bulk compressibility under normal stress exceeding the benefit achieved by such modified soil resisting the effects of shear stress. In this case (i.e. $h_{rs}/D > 0.4$), although the void ratio of mixture layer is kept constant (regardless of the thickness of the RSM layer), but with increase in the ratio of h_{rs}/D the total void spaces between the soil particles of mixture, the total density of foundation bed and compressibility of mixture are increased. The increase in the total density and compressibility of foundation bed could be linked with

the decrease in the unit weight and CBR values of gravel and tire buffings mixtures as the amount of tire buffings increases (Cabalar and Karabash, 2015). The results also suggest that an increase in the thickness of RSM beyond 0.8 times the loading surface diameter ($h_{rs}/D > 0.8$), which was not examined in the tests, might lead to more significant enhancement in settlement, particularly at high cyclic load levels. Therefore, it may also be expected that the behaviour of the mixture changes from a relevant and competent reinforcing material to a highly compressible material, which may provide no reinforcement effect, thereby causing an undesirable effect on the foundation response so that the performance of the foundation bed is reduced relative to that of the untreated bed. However, the effect of the h_{rs}/D values beyond 0.8 particularly as entire foundation should be investigated in future study.

The effect of the amplitude of the cyclic load on the settlement of the footing is also clear from Fig. 6. As expected, the increase in the cyclic load magnitude causes a direct increase in settlement of the foundation bed, irrespective of the thickness of mixture. Consider, for example from Fig. 6b the residual plastic settlements for the foundation bed with an optimum h_{rs}/D value of 0.4 ($h_{rs}/B = 0.4$). At the end of loading, the residual plastic settlements are 2.88, 6.84, 12.78, 18.97 and 28.94 mm for magnitudes of cyclic load of 140, 280, 420, 560 and 700 kPa, respectively. This example shows that the residual plastic settlement varies non-linearly with amplitude of load cycle (e.g., for the applied load of 140 and 280 kPa, the residual plastic settlement grew by a factor of about 2.40 whereas the amplitude of load cycle only doubled).

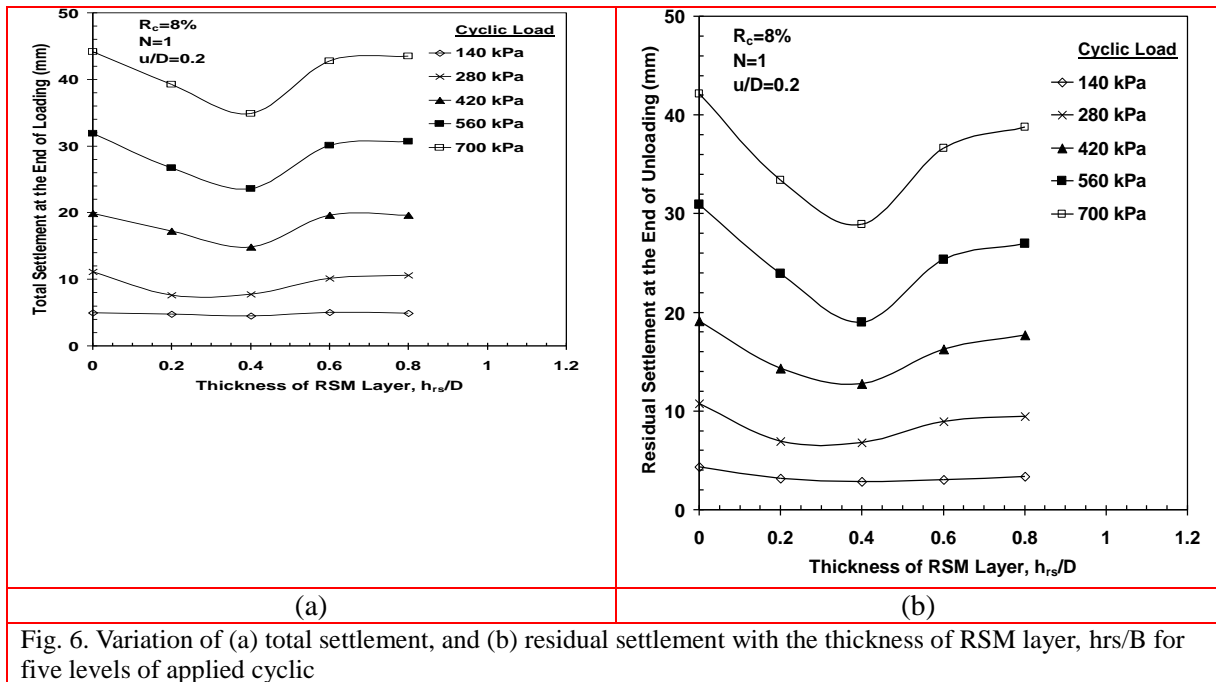


Fig. 6. Variation of (a) total settlement, and (b) residual settlement with the thickness of RSM layer, h_{rs}/B for five levels of applied cyclic

6.2. The effect of the number of rubber-soil mixture layers (N)

To investigate the beneficial effect of the number of RSM layers on the behaviour of foundation bed, Fig. 7 presents the pressure-settlement response of the foundation bed with none, one, two, and three layers of RSM ($N=0, 1, 2, 3$). The layers of RSM were employed at the optimum thickness revealed by Test Series 2, i.e. $h_{rs}/B=0.4$ with the same rubber content of 8% ($R_c=8\%$) and at the same placement spacing, $u/D=h/D=0.2$. The hysteresis behaviour seen in Fig. 7 is linked with a reduction in the total and residual settlements with increase in the number of mixture layers (i.e., the increase in the depth of the treated zone) at a given level of applied pressure. A possible explanation of the improved performance by the RSM layers is internal confinement which would restrict lateral displacement in the foundation bed, thereby limiting the settlement of the foundation. This internal confinement, also termed confinement reinforcement, was explained by [Yang in 1974](#). In the present study, it may be also attributed to the effect of tensile strength of the rubber particles and the friction at the soil-rubber interface. The behavioral patterns observed in these tests (e.g. Fig. 7) is in-line with those observed in the repeated load testing on granular material by several authors (e.g. [Pérez et al., 2006](#); [García-Rojo and Herrmann, 2005](#)). Also rubber-treated granular soil can be expected to perform better when subjected to a shear load, e.g. optimally at a depth of around 0.5-1 times the footing width where shear stresses are greatest (Boussinesq, 1885) than deeper depths when shear stresses are low – in which situations compression of the rubber can be expected to dominate performance.

In order to directly investigate the beneficial effect of multi-layered RSM in decreasing settlement, the variation in total and residual settlements of the foundation beds with RSM layers (extracted from Fig. 7) for different amplitudes of cyclic load are shown in Fig. 8. The results in Figs. 7 and 8 depict that, the maximum and residual settlements of the loading plate are considerably decreased relative to the deformation of the soil-only installation, regardless of the level of applied cyclic load. For example, from Fig. 8b at 700 kPa amplitude of applied cyclic load, the residual settlement values are about 42.13, 28.94, 21.64, and 20.41 mm for the soil-only bed, and beds with one, two and three layers of RSM, respectively. This example provides clear illustration how the rate of reduction in the residual plastic settlement (and also the total settlement, in Fig. 8a) reduces with increase in the number of RSM layers (N). It indicates about 49% and 51% reduction in residual settlement when three and four layers of RSM are used respectively compared to none. Similar results have been reported by [Moghaddas Tafreshi et al. \(2014\)](#) regarding improvements in the total and residual settlements with number of geocell layers and by [Thakur et al. \(2012\)](#) when the thickness of a single geocell layer increased in depth of reinforced bed.

Fig. 8 also illustrates that no marked further decrease in the total and residual settlements occurs when the third layer of RSM is added. Thus, it is evident that the strain at the depth of the third RSM layer is inadequate to mobilize any significant reinforcement benefit. Such a finding is not unexpected as a simple stress analysis (e.g. according to [Boussinesq \(1885\)](#)) will show that the zone of soil influenced by the footing loading (at ultimate capacity) only extends to a depth of $\approx 1-2$ times the footing width/diameter. Therefore marginal performance improvement in footing settlement would be expected when the value of N increase beyond 3 layers (i.e. when the lowest layer is located at below $1.4D-1.8D$) and thus 3 layers of RSM could be considered as the optimum layer number.

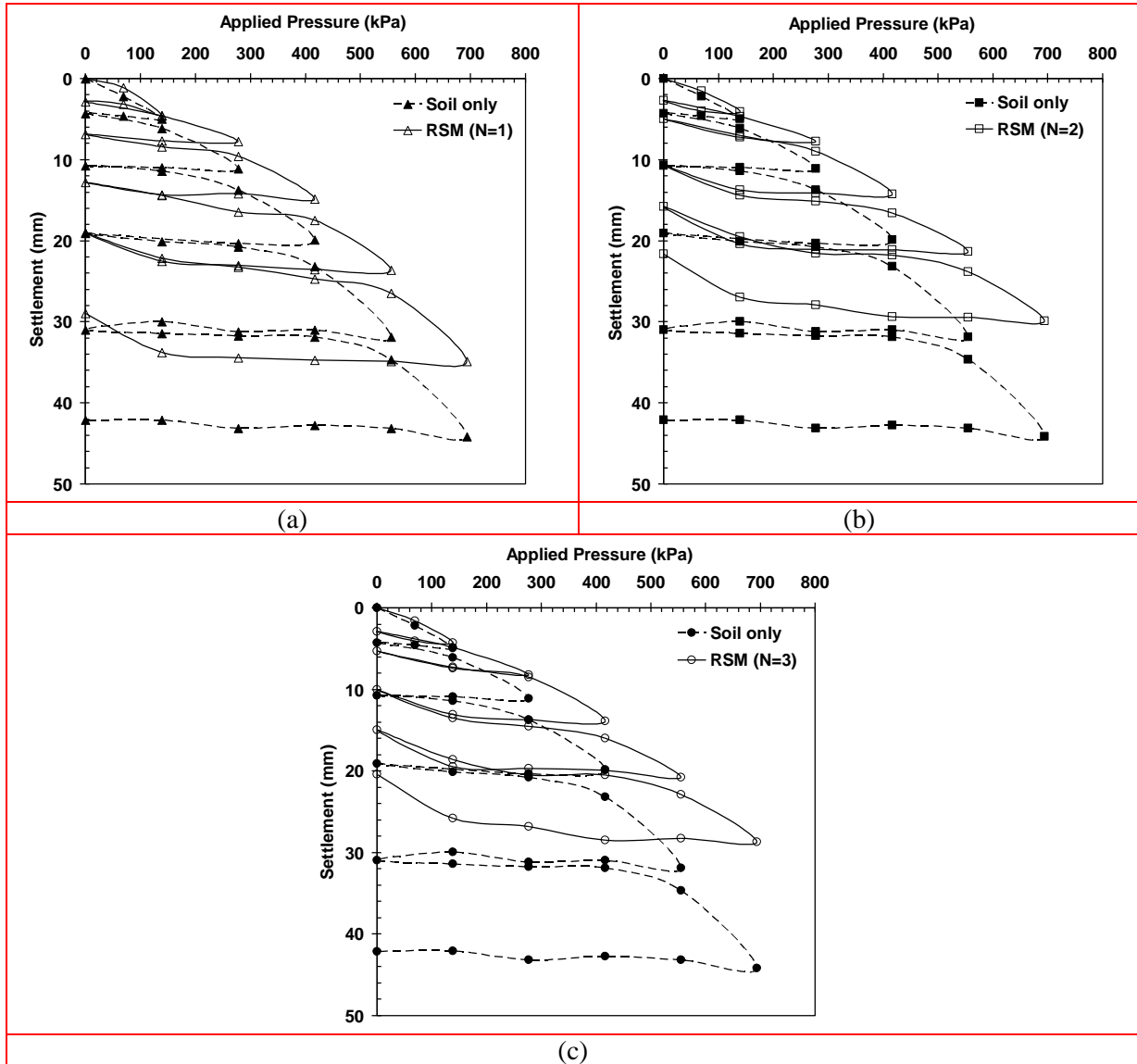


Fig. 7. Comparison of the pressure-settlement response of foundation beds with 0, 1, 2 and 3 RSM layers ($R_c=8\%$, $h_{rs}/D=0.4$, $h/D=0.2$ and $u/D=0.2$). (a) $N=1$, (b) $N=2$, (c) $N=3$.

Also, as expected, the increase in the magnitude of the cyclic loads causes the plate settlement to increase for all installations. Comparing the gradient of the lines in Fig. 8, it is evident that almost all the benefit at 140, 280 and 420 kPa surface loadings comes from the first RSM layer (the lines are essentially parallel beyond $N=1$). Only when the applied surface stress reaches 560 kPa or greater does

a difference appear in the gradient of the curve linking the $N=1$ and $N=2$ results. Thus, at lower applied stresses, all the effective benefit of the RSM is delivered when that material lies above $0.8D$. However, when higher stress (i.e. 560 and 700 kPa) is applied –the limiting depth for beneficial application is $1.4D$.

To the authors' knowledge, this is the first study of rubber-treated soil being placed as layers beneath a foundation, so it is not possible to make any direct comparisons with other researchers' studies. As a partial comparison, the results illustrated by Fig. 8 were compared with those of [Moghaddas Tafreshi et al. \(2013\)](#) who placed layers of geocell in a similar soil. The similarity of response is striking. This strongly suggests that the rubber does, indeed, have a reinforcing mechanism. However, the increasing settlement with thicker RSM layers (Fig. 6) and the concentration of the benefit with the first RSM layer (see previous paragraphs) suggests that the reinforcing benefit is opposed by a softening action caused by compressible rubber inclusions in the manner explained above in Section 6.1. Hence, some rubber is beneficial but too much is counter-productive. Parallel observations on the optimal rubber addition to a granular soil have been made, for example, by [Reddy et al. \(2016\)](#).

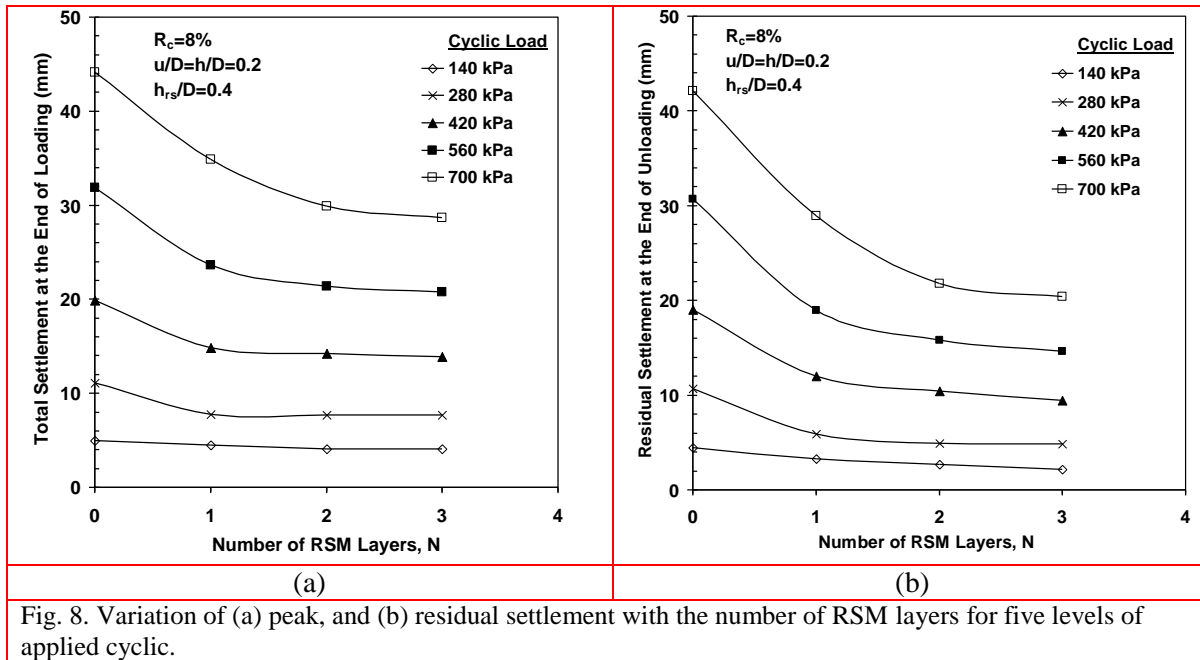


Fig. 8. Variation of (a) peak, and (b) residual settlement with the number of RSM layers for five levels of applied cyclic.

6.3. The pressure transferred in depth of foundation bed

The variation of pressure measured inside the soil-only bed and the RSM beds at the three levels of 210 mm ("SPC 1"), 390 mm ("SPC 2") and 570 mm ("SPC 3") beneath the center of the loading plate (see Fig. 3) is illustrated in Fig. 9. In this figure, the values of pressure measured at the peak of the load cycles of 280, 400, 560 and 700 kPa are given.

The plots reveal several features of the responses:

- a. The addition of an RSM layer above a stress monitoring point decreases the vertical stress significantly. For example compare the N=0 and N=1 responses with each other at 210 mm (just below the highest RSM layer); or compare the N=1 and N=2 readings at a depth of 390 mm (just below the second RSM layer). Therefore, adding an RSM layer can provide significant load spreading.
- b. The addition of RSM layers beneath a stress measuring point make no significant difference to the stress at the point. For example, compare the N=1, 2 and 3 readings to each other at a depth of 210 mm just below the highest RSM layer; or compare the N=2 and 3 readings at a depth of 390 mm (i.e. just below the second RSM layer) with each other. Thus, the stress at any depth is only affected by the construction above it and never by that below.
- c. Only at the higher surface stress levels do the lower RSM layers have any noticeable effect in reducing in-soil stress. For example, if the results for N=1 and N=2 at a depth of 390 mm under a surface pressure of 280 kPa are compared, it will be seen that there is little difference. However, a comparison of the same data when the surface pressure is 560 kPa reveals a noticeable difference. Similarly, the N=2 and N=3 results at a depth of 570 mm may be compared under the two surface pressures. For the 280 kPa surface stress, the in-soil stresses are the same whereas for the 560 kPa surface stresses the addition of a third RSM layer does have an effect. Thus, as discussed in Section 6.2, it is only at the higher applied stresses that any reinforcement benefit is obtained from deeper RSM layers. One might, alternatively, state this in terms of a RSM layer only providing reinforcing benefit once some, unquantified, threshold stress level has been exceeded.
- d. The pressure distribution is non-linear with stress. Probably this is due to the need for the stress in the RSM to rise to some threshold level before reinforcement effect, and thus load spreading, is provided. For example, consider the N=2 results at a depth of 390 mm. Beneath the center of loading the stresses are about 65 and 184 kPa for magnitudes of cyclic load that are 280 and 560 kPa, respectively. Thus, the distributed pressure grew by a factor of 2.83 whereas the amplitude of the load cycle only doubled.

Overall, it can be asserted that, when the layers of RSM are used at an optimum thickness and located at an optimum location inside the foundation bed, both stress reduction and vertical displacements reduce due to the provision of a composite system with modified shear strength. This mechanism, known as the “confinement effect” in the literature of soil reinforcement, allows the treated zone to act like a large mat that spreads the applied load over an extended area, instead of directly at the point of contact, and provides a composite slab with higher flexural stiffness ([Dash et al., 2003](#) and [Thakur et al. 2012](#) for geocell layer was placed in the foundation bed), higher modulus, and greater load support capabilities – consequently decreasing the distributed pressure at depth in the foundation bed.

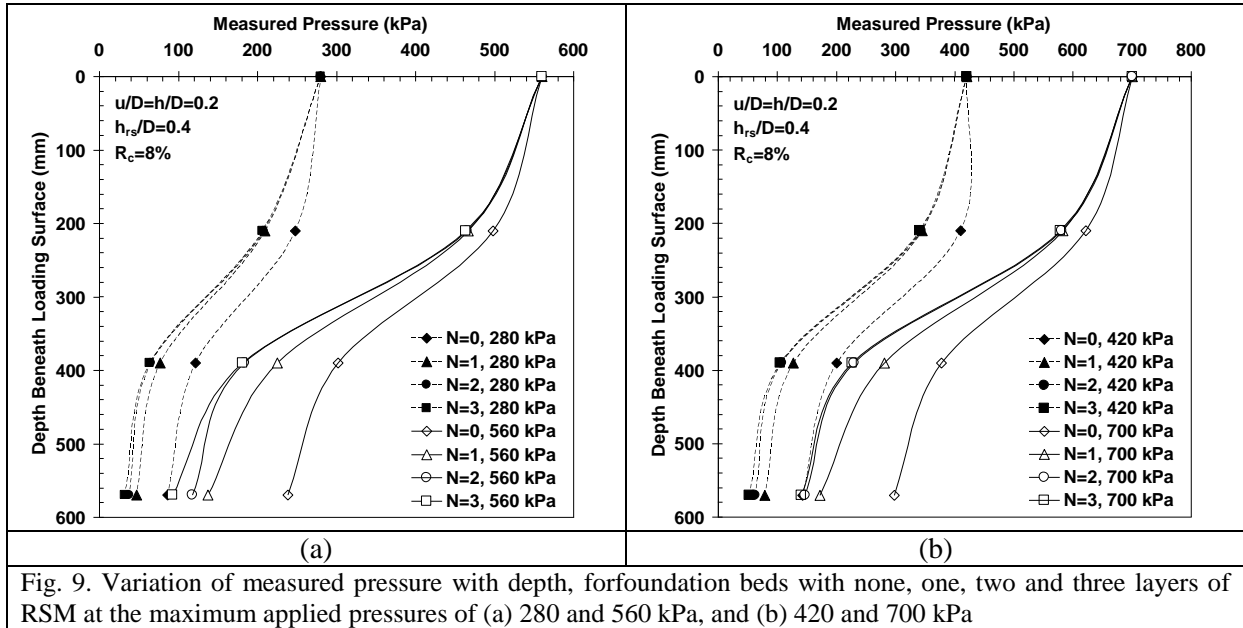


Fig. 9. Variation of measured pressure with depth, for foundation beds with none, one, two and three layers of RSM at the maximum applied pressures of (a) 280 and 560 kPa, and (b) 420 and 700 kPa

6.4. Resilient settlement and coefficient of elastic uniform compression of foundation bed

The elastic rebound corresponding to any pressure level of loading versus the amplitude of pressure can be plotted as shown in Fig. 10 for different number of RSM layers. This figure shows that, regardless of the magnitudes of cyclic pressure, the elastic rebound increases with increase in the number of RSM layers, indicating greater stored energy. For example, the elastic settlements during unloading from 560 kPa are about 1.19, 4.67, 5.57 and 6.14 mm for $N=0, 1, 2$ and 3 RSM layers, respectively. Thus more layers of RSM deliver greater resilience to the system, but the increases become less and less as the additional layers get further from the loading plate and, hence, contribute less benefit.

The trend lines in Fig. 10 are plotted from five data points corresponding to the five loading, unloading and reloading stages. The value of the coefficient of elastic uniform compression, CEUC, (in MPa/m) is the slope of trend line which can be calculated from Eq. 1 (Prakash, 1981).

$$CEUC = P/S_e \quad (1)$$

in which P =corresponding load intensity per square meter (MPa) and S_e =elastic rebound settlement (m) corresponding to the removal of load P .

Thus, the slope of elastic lines in Fig. 10 is representative of the CEUC (Prakash, 1981), which decreases with increase in the number of RSM layers inside the foundation bed, due to increase in the elastic settlement of the foundation beds. From this figure, the value of CEUC for beds with none, one, two and three layers of RSM were obtained as 397, 124, 94 and 88 MPa/m, respectively. Notice:

- the large reduction when rubber is first introduced (compared to the much smaller reductions when further rubber is added lower in the foundation),
- that, although each CEUC is treated as constant (a straight line on Fig. 10), the underlying data (the individual points in Fig. 10) show non-linearity with increased softness (less stiffness) at higher applied pressure.

Thus, the effect of the rubber in increasing the elastic settlement is clear and opposes the decrease in plastic settlements described earlier in the paper.

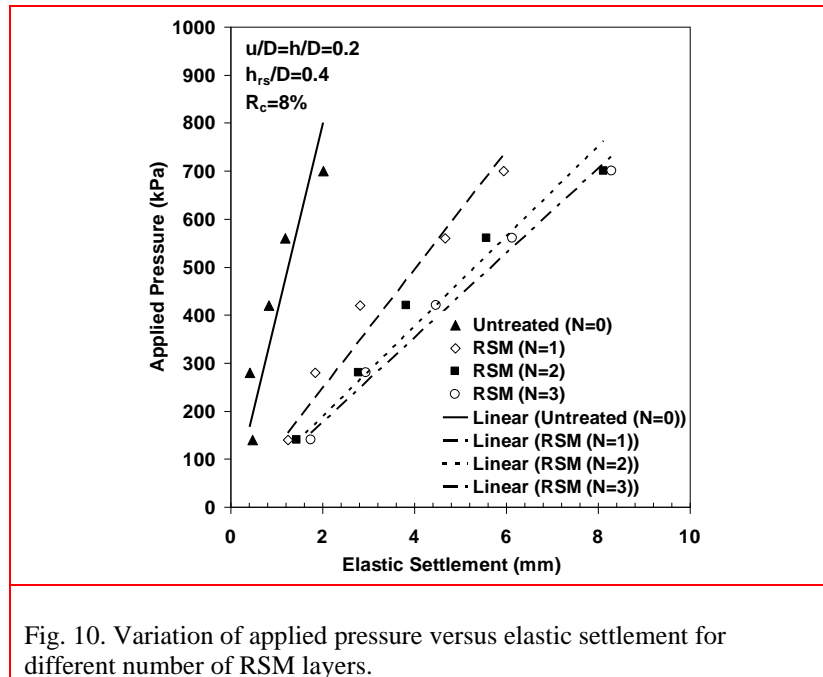


Fig. 10. Variation of applied pressure versus elastic settlement for different number of RSM layers.

7. Numerical Analysis

Finite difference analyses using [FLAC-3D \(2002\)](#) were performed to simulate and to investigate the behaviour of multi-layered RSM foundations under incremental cyclic loads. To calibrate and verify the multi-layered soil-rubber system, two different analyses were performed. The first was the analysis of a cylinder simulating a triaxial specimen as tested at the calibration stage (see Section 7.1 below). By this means the appropriate material properties for the numerical model were back-figured and these were then applied in the numerical model of the foundation beds containing RSM layers.

7.1. Model Calibration

As part of the calibration, six triaxial tests were performed to assess the properties of both untreated sand and of the RSM layers with 8% rubber ($R_c=8\%$ as optimal rubber content). The densities of the

soil and of the RSM were maintained for both the cyclic plate load tests and triaxial tests. Triaxial tests at three confining pressures of 50, 100 and 150 kPa were conducted. The triaxial samples had a diameter of 100 mm and a height of 200 mm. An elastic-perfectly plastic associative Mohr–Coulomb constitutive model was used to simulate the behaviour of soil and RSM specimens. Even though more sophisticated elasto-plastic constitutive models exist, the Mohr–Coulomb model is deemed satisfactory in the present case as the anticipated stress paths lead to stress-strain responses that are mainly dominated by shear failure when significant load is applied to the soil sample. To calibrate the parameters of the chosen plasticity model, the following points were considered:

- a) [Gotteland et al. \(2005\)](#) investigated some triaxial tests on rubber-soil mixture and found that, with an increasing proportion of rubber volume in samples, the trend of most specimens was to yield a decrease of both cohesion and friction angle.
- b) The dilation angle of all composites was assumed to be two-third of the value of friction angle in the same material as suggested by [Alimardani Lavasan and Ghazavi \(2008\)](#).
- c) "Mechanical local damping", a FLAC 3D option was employed in the numerical modelling as a way of allowing for energy loss as a result of internal friction and any slippage along interfaces.

To calibrate the parameters, the numerical model was used to replicate the triaxial tests on soil and RSM samples. By using a trial-and-error technique, adjusting the input parameters until the results of these numerical analyses closely matched those obtained from triaxial tests, representative values of bulk modulus (K), shear modulus (G), cohesion (c), friction angle (ϕ), dilation angle (ψ) and unit weight (γ) were obtained. Fig. 11 compares the stress-strain responses of untreated and samples containing rubber at confining pressures of 100, obtained in this way from the calibrated numerical simulations, with the experimental data measured from the same test configurations. As can be seen, there is generally a favorable match between the numerical results and the triaxial tests for both samples. The properties of the sand and the RSM (with 8% rubber inclusions by weight) to be used in the numerical analyses of the conventional and RSM foundations, are presented in Table 3. As seen in Table 3, the RSM layers have a greater value of cohesion (c) compared to that of the untreated soil, without any change in the value of the internal friction angle. These phenomena were observed by Zornberg et al. (2004) and Singh et al. (2016) using triaxial tests on rubber-soil mixtures. They reported no significant change in the internal friction angle (ϕ) and remarkable increase in cohesion of rubber-soil mixture compared to that of the unreinforced sand, which they explained in terms of significant interlocking effect.

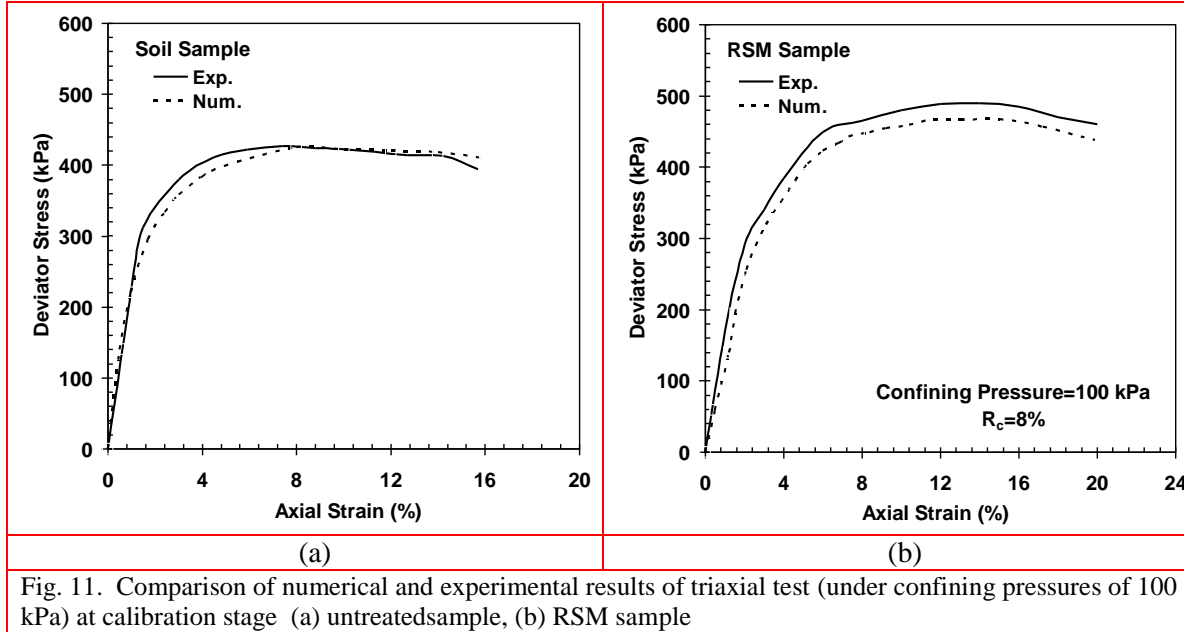


Fig. 11. Comparison of numerical and experimental results of triaxial test (under confining pressures of 100 kPa) at calibration stage (a) untreated sample, (b) RSM sample

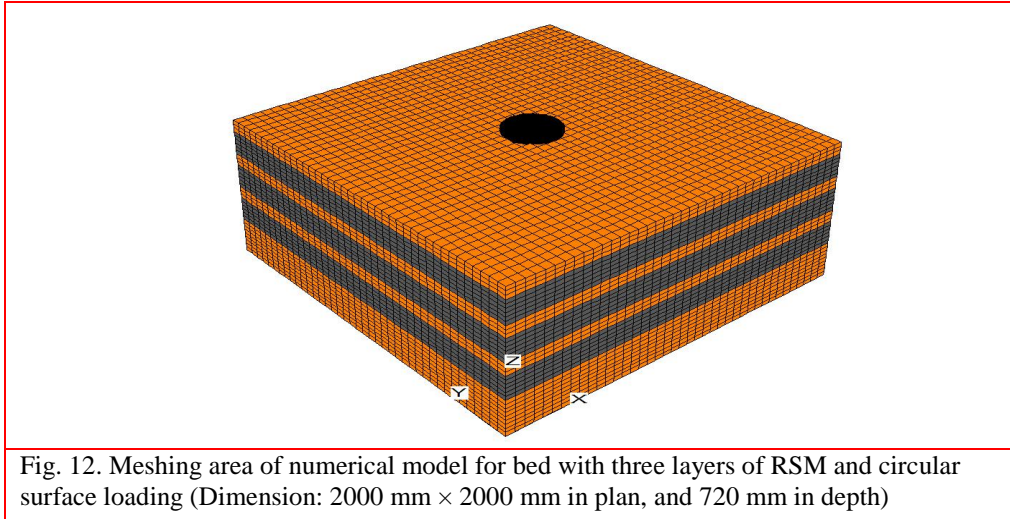
Type of material	K (MPa)	G (MPa)	C (kPa)	ϕ (Deg.)	ψ (Deg.)	γ (kN/m ³)
Untreated soil	9.7	3.9	6.5	34	7	18.52
Rubber treated soil ($R_c=8\%$)	6.3	3	20	34	5	13.60

7.2. Model Verification

After calibration, the materials with the characteristics presented in Table 3 were set to verify the simulated foundations. The dimensions of the simulated model replicated those of the experimental model (see Fig. 3). Fig. 12 shows meshing area of numerical model (e.g. for bed with three layers of RSM). The domain was divided into 17200 mesh 'openings' connected by 19866 grid points, organized in brick patterns. The outer boundaries were restrained horizontally while the base was restrained in all directions.

The loading plate is arranged so as to apply the load uniformly downward at the nodes immediately underneath the plate. This will not be an exact representation of reality but, given the deformability of the soil, should become close to reality after strains develop in the soil. Horizontal displacement at the interface between the loading plate and soil were restrained to zero, thereby simulating perfect roughness of the plate/soil interface. In the analysis, to simulate the plate loading, the vertical cyclic load was applied, and later removed, incrementally in 1.5 kPa steps so as to smoothly replicate the loading pattern in the cyclic plate load tests. Cyclic loading and unloading of the model continues until the response is stabilized and no more plastic deformation occurs, or until failure is observed (i.e. reducing load carrying capacity). Before applying the external load on the footing, the initial gravitational stress condition was established by attributing an initial stress state to the soil and RSM

layers at grid points. Stress in the vertical direction is equal to the product of the unit self-weight of the soil and the distance of the grid points from the surface.



To demonstrate the performance and accuracy of the numerical model to predict the behaviour of foundation beds under incremental cyclic loads, the comparison of the pressure-settlement variations of the foundation beds with no RSM layers (untreated bed) and with three RSM layers (N=3), as obtained from numerical analysis and experimental tests are shown in Fig. 13. This figure shows that the numerical results agree reasonably well with the experimental data. It also indicates that the numerical simulation is promising for estimating the behaviour of foundation bed under incremental cyclic load (loading, unloading and reloading) and may conveniently be used as a tool to evaluate the distribution of stress, displacement and strain throughout the foundation bed.

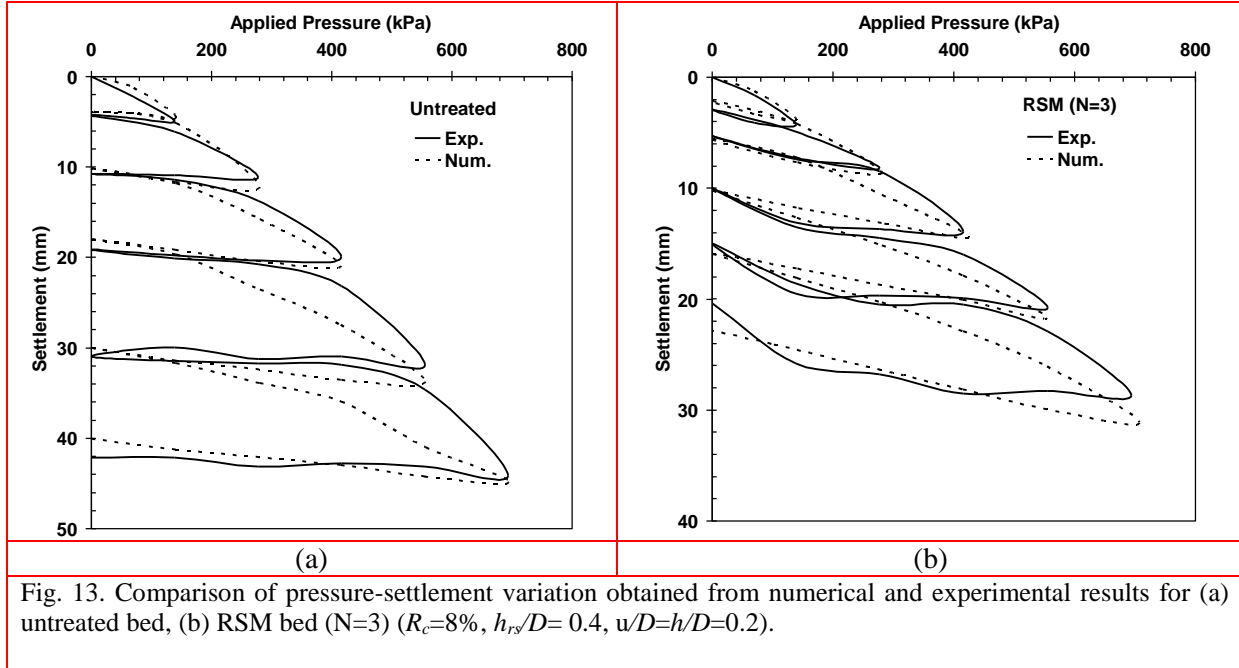
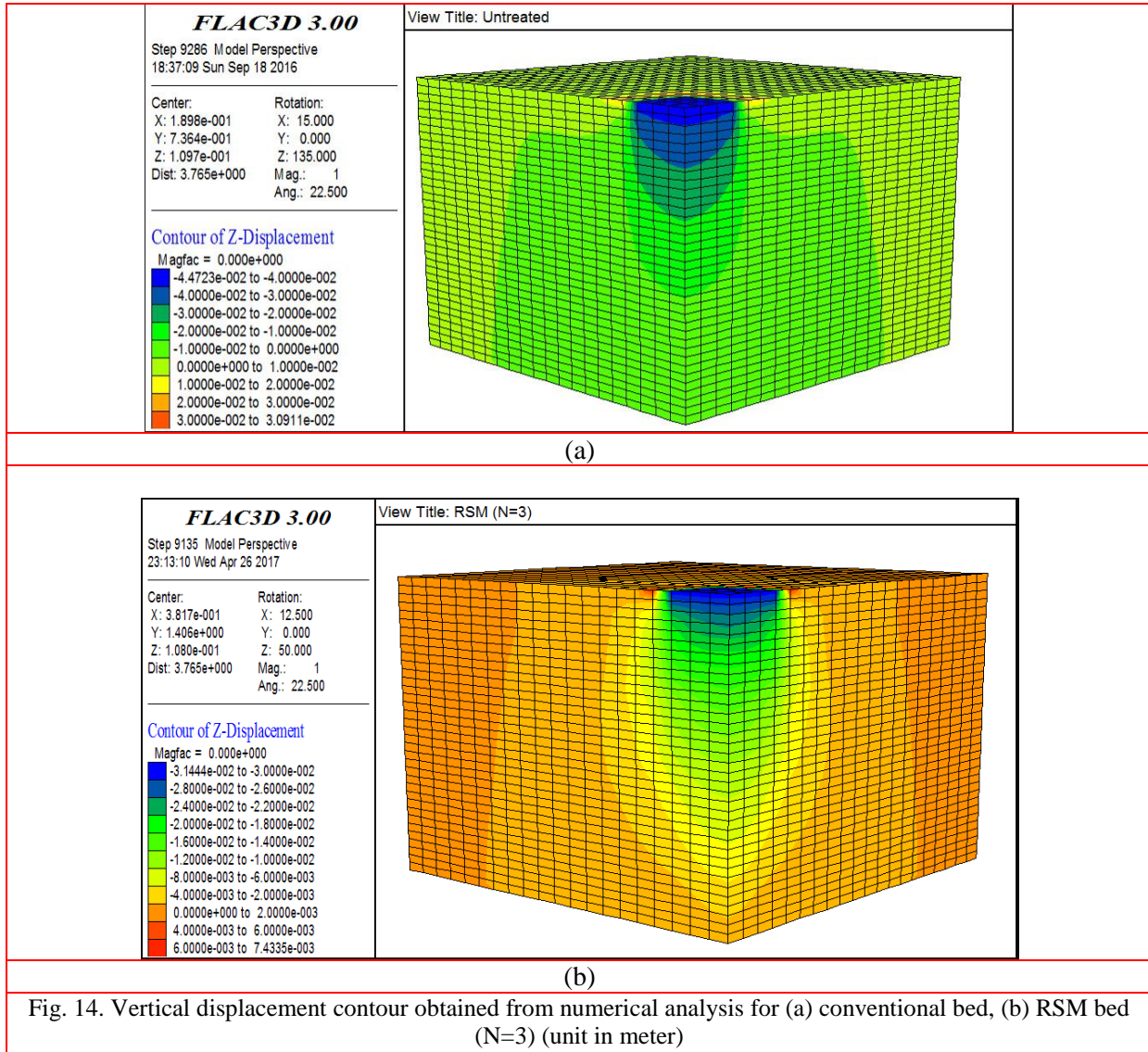


Fig. 13. Comparison of pressure-settlement variation obtained from numerical and experimental results for (a) untreated bed, (b) RSM bed (N=3) ($R_c=8\%$, $h_{rs}/D=0.4$, $u/D=h/D=0.2$).

7.3. Displacement and shear strain distributions

To assess the affect of RSM layers on deformation propagations within the foundation bed, Fig. 14 compares the vertical displacement contours for the conventional bed and the bed with three layers of RSM. The vertical displacement contours plotted correspond to the maximum load at the last loading cycle (i.e. 700 kPa cyclic loading). The negative values in z direction imply that the vertical settlement was happened in downward direction. The distribution of the displacement contours confirms the suitability of the boundary location in the physical test arrangements – it provides confidence that the footing settlement under incremental cyclic loads is not affected by boundary positions. The figure clearly shows the rapidly reducing magnitude of the vertical displacement across the depth.

The results in Fig. 14b show that the presence of three layers of RSM in the bed decreases deformation of foundation bed compared to the untreated bed in Fig. 14a (compare, for example, the position of the 2 cm displacement contour, which is at the dark green – mid green boundary in Figures 16a and 16b). A possible explanation is the expansion of the passive zones in an improved foundation due to the effectiveness of the confinement provided by rubber inclusions. In the untreated condition, part of the passive zone in the backfill has been lost, tending to lead to enhanced settlement compared with that of the treated bed (see Fig. 7c) and can be expected to allow the bed to deflect more.



The shear strain contours for the untreated bed and bed with three layers of RSM are shown in Fig. 15. As can be seen from this figure, the intensity of shear strains beneath the loading surface reduces by using RSM layers in the foundation bed (compare, for example, the position of the 10% strain contour, which is at the top of the dark blue boundary in Figure 15a and at the top of the mid green boundary in Figure 15b). Thus, the numerical analyses indicate that the failure shear mechanism has changed because of the RSM layers and that an enhancement in bearing capacity of the RSM bed has been achieved.

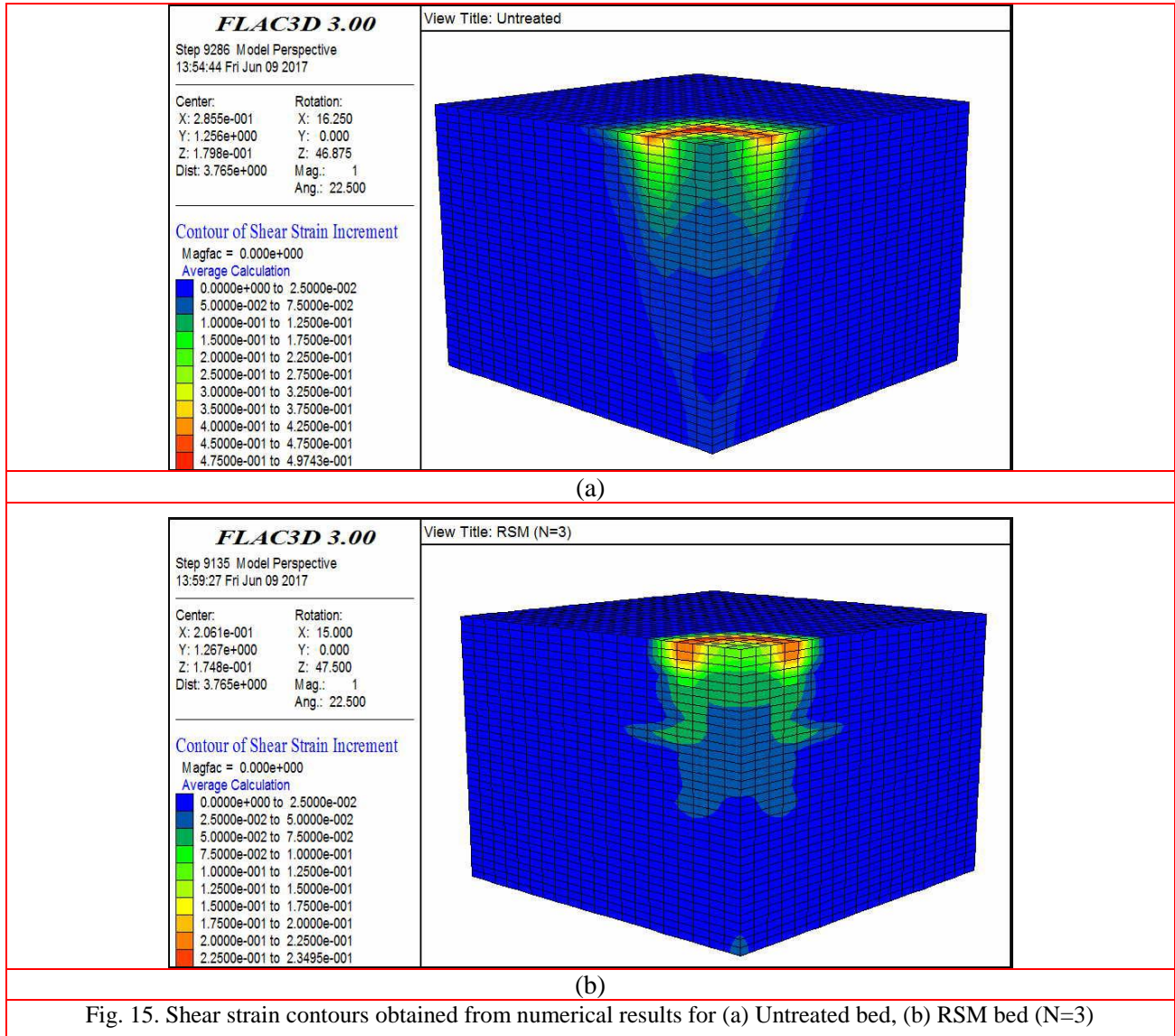


Fig. 15. Shear strain contours obtained from numerical results for (a) Untreated bed, (b) RSM bed (N=3)

8. Conclusion

Based on the results obtained from a series of incremental plate load tests of a sandy soil and of a bed containing several layers of rubber soil mixture, the following conclusions can be extracted:

(1) RSM layers are able to provide a reinforcing benefit similar in kind to that provided by a layer of geosynthetic or geocell reinforcement. In the absence of long fibers or continuous tensile members, the micro- or macro-scale mechanism(s) by which this is achieved is not clear.

(2) Increasing the amount of rubber in a RSM foundation layer increases compressibility and this behaviour opposes the reinforcement benefit. There is, therefore, an optimum amount of rubber for net improvement of foundation settlement responses.

(3) The optimum thickness of RSM layer, under incremental cyclic loads, based on plate settlement, is approximately 0.4 times the footing diameter ($h_{rs}/D \approx 0.4$).

(4) As the number of RSM layers increases, the footing settlement decreases due, in part, to better load spreading of the composite system. Under the last cycle of loading repeated in this paper (at 700 kPa with three layers of RSM (N=3)), the residual, plastic, deformation is only about 65% of the value for the conventional case.

(5) Under cyclic loading, use of the RSM layers is effective in reducing the stress distributed down into the foundation bed. At a depth of 390 mm (30 mm beneath the second of two layers of RSM), the vertical stress transferred from a cyclic surface load of 560 kPa is reduced by 39%, compared with the stress at the same point when no RSM layers are used.

(6) The coefficient of elastic uniform compression, CEUC decreases with the inclusion of RSM layers, the decrease being somewhat more for increasing the number of layers.

(7) The RSM layers increase the damping ratio by 4-5% beyond the value of 12-15% obtained on sand alone. This makes it, potentially, a very attractive material to achieve vibration attenuation for machine foundation and railway track beds.

(8) A numerical model, calibrated from laboratory unit cell tests was used to model the large-scale installations. Good agreement of the responses to loading was obtained. From the numerical analysis, it is deduced that the presence of soil-rubber layers can significantly reduce the deformation and vertical stress through the foundation bed as compared with the conventional bed.

The tests results are obtained for only one type of soil, one type and size of rubber, and one load diameter. In spite of these limitations, the plate load tests and the matching numerical simulations carried out in the present study provide considerable encouragement for the use of multi-layered RSM system with inter-layers of untreated soil, for addressing localized soft foundation conditions. Although, generalization may be needed before these findings may be directly applied, yet the results could be used in conducting large-scale model tests, and in further developing the analytical models. Using rubber derived from scrap tires as a soil-improvement agent has the potential to deliver considerable environmental and economic benefit, although economic assessments of the production and placement of soil-rubber mixtures at a commercial scale would need to be performed to assure users of the applicability of the findings in every situation. Therefore larger scale trials with a detailed economic and sustainability evaluation are recommended.

Acknowledgements

Dr. T. Amirsoleymani, the managing director of Mandro Consulting Engineers and their technicians provided the loading system, pit, some of the instrumentation and great assistance during the tests. The authors appreciate all the above support.

References

- Alimardani Lavason, A., Ghazavi, M., (2008). Influence of Interference on Failure Mechanism of Closely Constructed Circular Footings on Reinforced Sand. Proceedings of 4th Asian Regional Conference on Geosynthetics, 311-317, Shanghai, China.
- Ahmadi H, Hajjalilue-Bonab M (2012) Experimental and analytical investigations on bearing capacity of strip footing in reinforced sand backfills and flexible retaining wall. *Acta Geotech* 7(4):357–373
- ASTM D1195 (2009). Standard Test Method for Repetitive Static Plate Load Tests of Soils and Flexible Pavement Components, for Use in Evaluation and Design of Airport and Highway Pavements, ASTM International, West Conshohocken, PA, USA.
- ASTM D1196 / D1196M (2004) Standard Test Method for Nonrepetitive Static Plate Load Tests of Soils and Flexible Pavement Components, for Use in Evaluation and Design of Airport and Highway Pavements. ASTM International, West Conshohocken, PA, USA.
- ASTM D1557 (2012) Standard Test Methods for Laboratory Compaction Characteristics of Soil Using Modified Effort. ASTM International, West Conshohocken, PA, USA.
- ASTM D2487 (2011) Standard Practice for Classification of Soils for Engineering Purposes (Unified Soil Classification System). ASTM International, West Conshohocken, PA, USA.
- ASTM D422 (2007) Standard Test Method for Particle-Size Analysis of Soils. ASTM International, West Conshohocken, PA, USA.
- Attom, M.F. (2006). The use of shredded waste tires to improve the geotechnical engineering properties of sands. *Environmental Geology*, **49** (4), 497–503.
- Boussinesq, J. (1885). Application des potentiels a l'étude de l'équilibre et du mouvement des solides élastiques, Albert Blanchard, Paris (in French). [Reprinted, 1969 with an introduction by A. Caquot, Gauthier-Villars, Paris.]
- Bosscher, P.J., Edil, T.B., Kuraoka, S., 1997. Design of highway embankments using tire chips. *J. Geotechnical & Geoenvironmental Eng'g*, ASCE, **123** (4), 295–304.
- Brara, A., Brara, A., Daouadji, A., Bali, A., Daya, El. M., (2016). Dynamic properties of dense sand-rubber mixtures with small particles size ratio. *European Journal of Environmental and Civil Engineering*, 1-15.
- Cabalar, A. F., Karabash, Z., 2015. California Bearing Ratio of a Sub-Base Material Modified With Tire Buffings and Cement Addition. *Journal of Testing and Evaluation* 43 (6).
- Cetin, H., Fener, M., Gunaydin, O. 2006. Geotechnical properties of tire-cohesive clayey soil mixtures as a fill material. *Engineering Geology*, **88** (1-2) 110–120.
- Chiu, C.T., 2008. Use of ground tire rubber in asphalt pavements: field trial and Evaluation in Taiwan. *J. Resources, Conservation & Recycling*, **52** (3), 522–532.
- Dammala, P., Reddy, B.S., Murali Krishna, A., 2015. Experimental Investigation of Applicability of SandTire Chip Mixtures as Retaining Wall Backfill, *IFCEE 2015*, 1420-1429. *Doi: 10.1061/9780784479087.128*.
- Dash, S.K, Sireesh, S, Sitharam, T.G., 2003. Model studies on circular footing supported on geocell reinforced sand underlain by soft clay. *Geotextiles and Geomembranes*, **21** (4), 197–219.
- Demir, A., Yildiz, A., Laman, M., Ornek, M., (2014) Experimental and numerical analyses of circular footing on geogrid-reinforced granular fill underlain by soft clay. *Acta Geotech* 9(4):711–723(4):357–373
- Edinçliler, A., Baykal, G., Dengili K., 2004. Determination of static and dynamic behavior of recycled materials for highways. *Resources Construction & Recycling*, **42** (3), 223-237.
- Edinçliler, A., Cagatay, A., 2013. Weak subgrade improvement with rubber fibre inclusions. *Geosynthetics International*, **20** (1), 39-46.
- Feng, Z.Y., Sutter, K.G., 2000. Dynamic properties of granulated rubber sand mixtures. *Geotechnical Testing J.*, **23** (3), 338–344.
- Finn, WD, Liam, Lee KW, Martin, GR., 1977. 'An effective stress model for liquefaction, *J. Geotechnical Eng'g. Div.*, ASCE, **103** (6), 517–33.

- FLAC-3D, Fast Lagrangian Analysis of Continua in Three dimensions 2002. ITASCA Consulting Group, Inc., Minneapolis, MN.
- García-Rojo, R., Herrmann, H.J., 2005. Shakedown of unbound granular material. *Granular Matter*, **7** (2), 109-118.
- Gotteland, P., Lambert, S., Balachowski, L. 2005, Strength characteristics of tyre chips-sand mixtures, *Studia Geotechnica & Mechanica*, **XXVII** (1-2), 55-66.
- Hataf, N., Rahimi, M.M., 2005. Experimental investigation of bearing capacity of sand reinforced with randomly distributed tire shreds. *Construction & Building Materials*, **20** (10), 910-916.
- Karabash, Z., Cabalar, A. F., 2015. Effect of tire crumb and cement addition on triaxial shear behavior of sandy soils. *Geomechanics and Engineering, An International Journal*. 8(1), 1-15.
- Keskin, M. S., Laman, M., 2014. Experimental study of bearing capacity of strip footing on sand slope reinforced with tire chips, *Geomechanics and Engineering, An International Journal*. 6(3), 249-262.
- Lee, C.J., Sheu, S.F. 2007. The stiffness degradation and damping ratio evolution of Taipei Silty Clay under cyclic straining. *Soil Dynamics & Earthquake Eng. J.*, **27**, 730–740.
- Masing G. Eigenspannungen & Verfestigung beim Messing, 1926. Proceedings of the second international congress of applied mechanics, Zurich, Switzerland.
- MathWorks Inc., (1999). MATLAB the Language of Technical Computing. Version 6, Natick, MA, USA.
- Moghaddas Tafreshi, S. N., Tavakoli Mehrjardi, Gh., Dawson, A. R., 2012. Buried Pipes in Rubber-Soil Backfilled Trenches under Cyclic Loading, ASCE, *J. Geotechnical & Geoenvironmental Eng'g.*, **138** (11), pp. 1346-1356.
- Moghaddas Tafreshi, S.N., Norouzi, A.H. 2012. Bearing capacity of a square model footing on sand reinforced with shredded tire – An experimental investigation. *Construction & Building Materials*, **35** (October), 547–556.
- Moghaddas Tafreshi, S.N., Khalaj, O., Dawson, A.R., 2013. Pilot-scale load tests of a combined multi-layered geocell and rubber-reinforced foundation. *Geosynthetics International*, **20** (3), 143–161.
- Moghaddas Tafreshi, S.N., Khalaj, O., Dawson, A.R., 2014. Repeated loading of soil containing granulated rubber and multiple geocell layers. *Geotextiles & Geomembranes*, **42** (1), 25-38.
- Moghaddas Tafreshi, S.N., Norouzi, A.H. 2015. Application of waste rubber to reduce the settlement of road embankment, *Geomechanics & Engineering*, **9** (2), 219-241.
- Munnoli, P.M., Sheikh, S., Mir, T., Kesavan, V., Jha, R. 2013. Utilization of rubber tyre waste in subgrade soil. *Global Humanitarian Technology Conference, South Asia Satellite (GHTC-SAS)*, 330-333.
- Nakhaei, A., Marandi, S.M., Sani Kermani, S., Bagheripour, M.H., 2012. Dynamic properties of granular soils mixed with granulated rubber. *Soil Dynamics and Earthquake Engineering*, **43** (6), 124-132.
- Newmark N.M., and Rosenblueth E., 1971. Fundamentals of earthquake engineering. Englewood Cliffs, NJ: Prentice-Hall, Inc., pp. 162–3.
- Pérez, I., Medina, L., Romana, M.G., 2006. Permanent deformation models for a granular material used in road pavements. *Construction & Building Materials*, **20** (9), 790-800.
- Prakash, S., 1981. Soil dynamics, New York, McGraw-Hill.
- Prasad, D.S.V., Prasada Raju, G. V. R., 2009. Performance of waste tyre rubber on model flexible pavement. *ARPN, J. Engineering & Applied Sciences*, **4** (6), 89-92.
- Recycling Research Institute, RRI., 2009. Online available from: <http://www.scraptirenews.com> (Accessed on 30th May 2011).
- Reddy, B.S., Murali Krishna, A., 2015. Recycled Tire Chips Mixed with Sand as Lightweight Backfill Material in Retaining Wall Applications: An Experimental Investigation. *Int. J. of Geosynth. and Ground Eng.* doi:10.1007/s40891-015-0036-0.

- Reddy, B.S., Pradeep Kumar, D., Murali Krishna, A., 2016. Evaluation of the Optimum Mixing Ratio of a Sand-Tire Chips Mixture for Geoenvironment Applications, *Journal of Material in Civil Eng.*, ASCE, **28** (2).
- Reddy, B.S., Murali Krishna, A., 2016. Mitigation of dynamic loading effects on retaining walls using recycled tire chips, *Indian Geotechnical Conference IGC2016*.
- Richard RM, Abott, B.J., 1975. Versatile elastic-plastic stress-strain formula. *J. Eng'g. Mech. Div.*, ASCE, **101** (4), 511-5.
- Rubber Manufacturers Association, RMA., 2007. Online available from: <http://www.rma.org> (Accessed on 30th May 2011).
- Singh, M., Mathur, A.M., Goswami, A., Pareek, C.P., Sachdeva, D., 2016. Effect on Shear Strength Parameters of Granular Soil of Rajasthan by Mixing Waste Rubber Fiber, *SSRG International Journal of Civil Engineering*, **3** (5), 2348 – 8352.
- Sitharam, T.G., Sireesh, S., 2005. Behavior of embedded footings supported on geogrid cell reinforced foundation beds, *Geotechnical Testing J.*, **28** (5), 452-463.
- Thakur, J.K., Han, J., Pokharel, S.K., Parsons, R.L., 2012. Performance of geocell-reinforced recycled asphalt pavement (RAP) bases over weak subgrade under cyclic plate loading. *Geotextiles & Geomembranes*, **35** (December), 14-24.
- Waste and Resources Action Programme, WRAP., 2005. Tyres re-use and recycling. Online available from: <http://www.wrap.org.uk>. (Accessed on 30th May 2011).
- Yang, Z. 1974, Strength and Deformation Characteristics of Reinforced Sand. Ph.D Thesis, University of California, Los Angeles, USA.
- Yoon, S., Prezzi M., Siddiki, N. Z., Kim, B., 2006. Construction of a test embankment using a sand-tire shred mixture as fill material. *Waste Management*, **26** (9), 1033-1044.
- Yoon, Y. W., Heo, S. B., Kim, S. K., 2008. Geotechnical performance of waste tires for soil reinforcement from chamber tests. *Geotextiles & Geomembranes*, **26** (1), 100-107.
- Zheng-Yi, F., Sutter, K. G. (2009). Dynamic Properties of Granulated Rubber/Sand Mixtures, *Geotechnical Testing J.*, **23**(3), 338-344.
- Zornberg, J.G., Cabral, A.R Viratjandr, C., 2004. Behaviour of tire shred-sand mixtures, *Canadian Geotechnical Journal*, **41** (2), 227-241.

LIST OF SYMBOLS

Nomenclature

b	Width of the RSM layers
c	Cohesion of soil
C_u	Coefficient of uniformity
C_c	Coefficient of curvature
D	Loading plate diameter
D_{10}	Effective grain size (mm)
D_{30}	Diameter through which 30% of the total soil mass is passing (mm)
D_{60}	Diameter through which 60% of the total soil mass is passing (mm)
G	Shear modulus of soil
G_s	Specific gravity of soil
h	Vertical spacing of the RSM layers
h_{rs}	Height of the rubber-soil mixture layers

h_s	Specified depth of the foundation
K	Bulk modulus of soil
N	Number of RSM layers
R_c	Rubber content
s	Settlement
u	Embedded depth of the first layer of RSM
γ	Soil density
ψ	Dilation angle
ϕ	Angle of frictional resistance of soil
RSM	Rubber Soil Mixture
SPC	Soil pressure cell
$SPC 1$	Top Soil Pressure Cell
$SPC 2$	Middle Soil Pressure Cell
$SPC 3$	Bottom Soil Pressure Cell
$q_{cycl.}$	Cyclic Pressure
$CEUC$	Coefficient of Elastic Uniform Compression,
P	Load Intensity per Area
S_e	Elastic Rebound Settlement